

creativecommons.org/licenses/by-nc-nd/4.0/

Peculiarities in the electrical and magnetic properties of cobalt perovskites $\text{Ln}_{1-x}\text{M}_x\text{CoO}_3$ (Ln^{3+} : La^{3+} , M^{2+} : Ca^{2+} , Sr^{2+} , Ba^{2+} ; Ln^{3+} : Nd^{3+} , M^{2+} : Sr^{2+})

M.A. Señarís Rodríguez^a, M.P. Breijo^b, S. Castro^a, C. Rey^a, M. Sánchez^a, R.D. Sánchez^b, J. Mira^c, A. Fondado^c, J. Rivas^c

^a Dpt. Química Fundamental e Industrial, Universidad de A Coruña, 15071 A Coruña, Spain

^b U.A. Tecnología de Materiales y Dispositivos, Centro Atómico de Bariloche, 8400 San Carlos de Bariloche, Argentina

^c Dpt. Física Aplicada, Universidad de Santiago de Compostela, 15706 Santiago de Compostela, Spain

International Journal of Inorganic Materials

Volume 1, Issues 3–4, September–October 1999, Pages 281–287

Available online 29 October 1999

doi:10.1016/S1466-6049(99)00042-2

Abstract

We refer here to the electrical and magnetic properties of the $\text{Ln}_{1-x}\text{M}_x\text{CoO}_3$ systems (Ln^{3+} : La^{3+} , M^{2+} : Ca^{2+} , Sr^{2+} , Ba^{2+} ; Ln^{3+} : Nd^{3+} , M^{2+} : Sr^{2+}), paying special attention to those ferromagnetic compounds that display M–I transitions as temperature rises: $\text{La}_{1-x}\text{M}_x\text{CoO}_3$ (M^{2+} : Ca^{2+} , Sr^{2+} , Ba^{2+}) in the compositional interval $x=0.2$ – 0.3 , and $\text{Nd}_{1-x}\text{Sr}_x\text{CoO}_3$, with $x=0.40$. The magneto-transport properties of such materials are peculiar and interesting: they show diodic behavior and large relaxation effects — these latter being specially important in the Nd compound — they display

magnetoresistive effects specially at the M–I transition temperatures, and they age with time. All these results are discussed on the basis of the inhomogeneous electronic structure of these doped cobalt perovskites and taking into account the influence of the lanthanide ion on their magnetic and electrical properties.

Keywords

A. oxides; D. electrical properties; D. magnetic properties

1. Introduction

The interplay between magnetism and electrical conductivity in perovskite-type oxides has been a matter of study in the last decades [1] and with renewed interest since the discovery of colossal magnetoresistance (CMR) in doped manganese-based compounds [2] and [3].

Within this family of compounds, cobaltites constitute another specially interesting system in view of the peculiar way their magnetic and electrical properties change with temperature and upon doping [4], [5], [6],[7] and [8], and more recently in view of the magnetoresistive effects found in $\text{La}_{1-x}\text{MxCoO}_3$ (M= Sr, Ba) systems [9], [10] and [11].

Early work on the undoped LaCoO_3 compound [4] established the existence of a thermally induced spin transition at the Co ions responsible for its peculiar behavior [5]. Since then many studies have tried to elucidate in more detail the characteristics of such transition, not only in LaCoO_3 [12], [13], [14] and [15] but also in other LnCoO_3 (Ln=rare earths) compounds [13], [16], [17] and [18].

Those early studies also showed that while LaCoO_3 shows high resistivity and antiferromagnetic exchange interactions, upon doping the $\text{La}_{1-x}\text{SrxCoO}_3$ materials evolve towards a ferromagnetic metallic behavior[6]. Since then, the magnetic and electrical properties of the $\text{La}_{1-x}\text{SrxCoO}_3$ system have been repeatedly investigated, finding that the evolution takes place smoothly, and that a number of different magnetic and electrical behaviors are present for the different degrees of doping: superparamagnetism, spin-glass/cluster-glass behaviors, etc., semiconducting/metallic behaviors, and even metal–insulator transitions as a function of temperature [7] and [19].

Those studies have also been extended to Ca- and Ba-doped $\text{La}_{1-x}\text{MxCoO}_3$ (M=Ca, Ba) materials [8] and [11], and to other $\text{Ln}_{1-x}\text{MxCoO}_3$ systems (Ln=rare earths) [8] and [20] that similarly show interesting electrical and magnetic properties.

Although the general trend in these $\text{Ln}_{1-x}\text{MxCoO}_3$ series of compounds (Ln=La, rare earth, M=Ca, Sr, Ba) is again that the materials tend to metallic and ferromagnetic behavior as x increases, the characteristics of that evolution depends on the nature of the lanthanide ion [8] and [20] and the nature of the dopant [8]. And while the properties of the end members of the systems seem to be well established, different magnetic and electrical behaviors have been reported for the intermediate members of the series [7], [8] and [19].

It is in that intermediate compositional range that we have focused our studies. And in this paper we report peculiar magneto-transport properties exhibited by certain $\text{Ln}_{1-x}\text{MxCoO}_3$ (Ln^{3+} : La^{3+} , M^{2+} : Ca^{2+} , Sr^{2+} , Ba^{2+} ; Ln^{3+} : Nd^{3+} , M^{2+} : Sr^{2+}) samples with x in the range 0.2–0.4 for which we find ferromagnetic behavior and metal-insulator transitions as temperature rises.

2. Experimental

$\text{La}_{1-x}\text{MxCoO}_3$ (M=Ca, Sr, Ba) and $\text{Nd}_{1-x}\text{SrxCoO}_3$ were prepared by decomposition of the corresponding mixture of nitrates.

Stoichiometric amounts of dry $\text{La}_2\text{O}_3/\text{Nd}_2\text{O}_3$, $\text{CaCO}_3/\text{SrCO}_3/\text{BaCO}_3$ and $\text{Co}(\text{NO}_3)_2$ were dissolved in nitric acid. The resulting solution was gently warmed up so as to slowly evaporate the solvent. The so-obtained mixture of nitrates was decomposed at 600°C. The resulting products were pressed into pellets and annealed at temperatures ranging from 970°C, for the $\text{Nd}_{1-x}\text{SrxCoO}_3$ series, up to 1175°C, for the $\text{La}_{1-x}\text{CaxCoO}_3$ samples. In all cases, after the thermal treatment at high temperatures, the samples were cooled slowly to room temperature (0.7°/min).

The product materials were examined by X-ray powder diffraction with a Siemens D-5000 diffractometer and $\text{Cu K}\alpha=1.5418 \text{ \AA}$ radiation. The morphology and size of the particles were studied in a scanning electron microscope (SEM) Jeol 6400.

Thermogravimetric analyses (TGA) and iodometric titrations under an argon atmosphere were carried out to study the oxygen content of the samples.

Magnetic properties were studied in a DMS-1660 Vibrating-Sample Magnetometer. Zero-field cooled (ZFC) and field cooled (FC) magnetic susceptibility data were obtained in a field of 1000 Oe from 77 to 330 K. ZFC magnetization curves $M(H)$ were obtained with fields ± 10 kOe at 77 K.

The electrical resistivity ρ was measured as a function of temperature in the range $77 < T \leq 300$ K in a zero magnetic field ($H=0$) and with a constant field ($H=5$ kOe) with a dc four-probe method using silver paint contacts. These contacts were renewed or even replaced by four new indium contacts or gold sputtered on to the samples, and the measurements repeated when detecting anomalous changes in the resistivity of the samples, in order to discard effects between sample and electrical contacts. The resistivity data were obtained, as commonly done, by calculating the averages ρ^+ and ρ^- (+ and - stand for the directions of the current) out of 10 values, respectively, and getting an average resistance $\rho = (\rho^+ + \rho^-)/2$. But in some cases, as it will be shown below, only one polarity of the current was used for the experiments, thus measuring either ρ^+ or ρ^- .

The magnetoresistance of the samples was measured between 0 and 9 kOe, specially at those temperatures at which the $\rho(H)$ vs. T curves, corresponding to $H=0$ and $H=5$ kOe, showed bigger separation.

3. Results

3.1. Sample characterization

According to their X-ray diffraction patterns, the following compounds were obtained as single-phase crystalline materials: $\text{La}_{1-x}\text{Ca}_x\text{CoO}_3$ and $\text{La}_{1-x}\text{Ba}_x\text{CoO}_3$ for $0 \leq x \leq 0.30$; $\text{La}_{1-x}\text{Sr}_x\text{CoO}_3$ for $0 \leq x \leq 0.50$; $\text{Nd}_{1-x}\text{Sr}_x\text{CoO}_3$ for $0 \leq x \leq 0.40$.

These results also show that in the $\text{La}_{1-x}\text{M}_x\text{CoO}_3$ samples, the introduction of the divalent ions progressively reduces the rhombohedral distortion present in the parent LaCoO_3 compound and increases the volume of the unit cell, in good agreement with data reported in the literature [6] and [8]. In the case of the $\text{Nd}_{1-x}\text{Sr}_x\text{CoO}_3$ system, for $0 \leq x \leq 0.40$ the compounds have all cubic perovskite structures with $a \approx 2a_c$, the cell parameter increasing with x .

As for the particle size and morphology of these samples, SEM micrographs show that, while $\text{La}_{1-x}\text{Sr}_x\text{CoO}_3$ and $\text{Nd}_{1-x}\text{Sr}_x\text{CoO}_3$ consist of small spherical particles of average

size $d \approx 0.5 \mu\text{m}$, in the Ca- and Ba-doped compounds, due to the higher temperatures used in their synthesis, sintering between particles has already taken place, resulting in plaquets 3.5 and 2 μm long, respectively.

3.2. Magnetic results

Upon substitution of the trivalent La^{3+} or Nd^{3+} ions by the divalent $\text{M}=\text{Sr}^{2+}$, Ca^{2+} , Ba^{2+} ions, the $\text{La}_{1-x}\text{MxCoO}_3$ and $\text{Nd}_{1-x}\text{SrxCoO}_3$ materials evolve towards ferromagnetic behavior.

The critical x to achieve magnetic percolation is $x=0.20$ in the case of the $\text{La}_{1-x}\text{SrxCoO}_3$, $\text{La}_{1-x}\text{BaxCoO}_3$ and $\text{Nd}_{1-x}\text{SrxCoO}_3$ systems, while it increases to $x=0.30$ in the $\text{La}_{1-x}\text{CaxCoO}_3$ series.

The Curie temperatures vary from system to system, although within each series T_c increases only very slowly with x , so that: $T_c(\text{La}_{1-x}\text{CaxCoO}_3) \approx 145$ K, $T_c(\text{La}_{1-x}\text{BaxCoO}_3) \approx 175$ K, $T_c(\text{La}_{1-x}\text{SrxCoO}_3) \approx 250$ K, $T_c(\text{Nd}_{1-x}\text{SrxCoO}_3) \approx 225$ K (Fig. 1a–d).

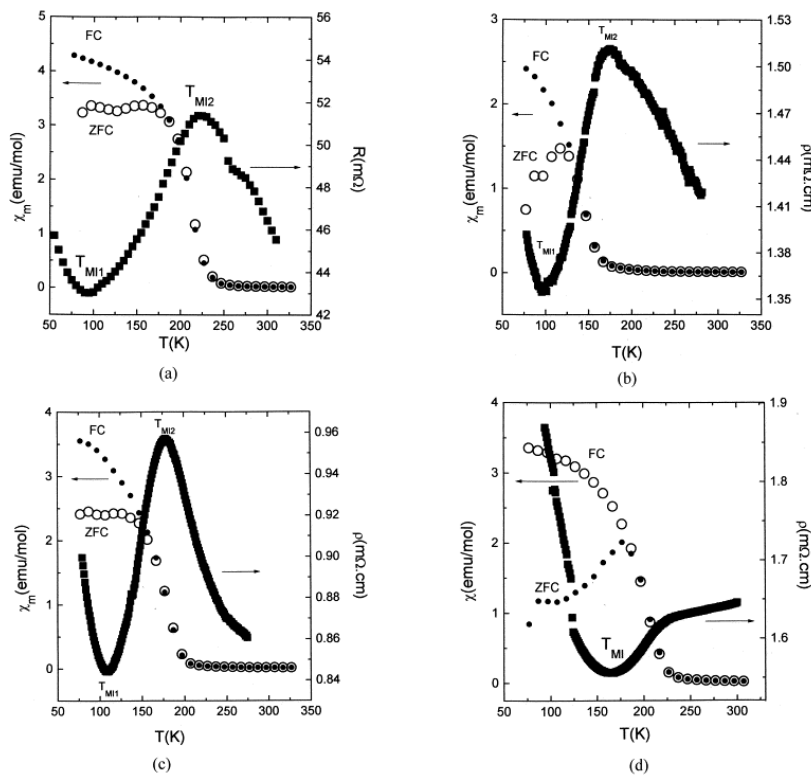


Fig. 1. Temperature dependence of the ZFC and FC molar magnetic susceptibility and the electrical resistivity of (a) $\text{La}_{0.75}\text{Sr}_{0.25}\text{CoO}_3$, (b) $\text{La}_{0.70}\text{Ca}_{0.30}\text{CoO}_3$, (c) $\text{La}_{0.80}\text{Ba}_{0.20}\text{CoO}_3$, and (d) $\text{Nd}_{0.70}\text{Sr}_{0.30}\text{CoO}_3$ samples

The $\chi(T)$ data follow a Curie–Weiss law for $\approx 250 \text{ K} < T < 330 \text{ K}$. From the corresponding $\chi^{-1}(T)$ fittings we can obtain information about how the effective magnetic moment per cobalt ion ($\mu_{\text{eff-Co}}$) and the Weiss constant (θ) are evolving with x in the different $\text{Ln}_{1-x}\text{MxCoO}_3$ series.

In the case of the $\text{La}_{1-x}\text{MxCoO}_3$ ($\text{M}=\text{Sr}, \text{Ca}, \text{Ba}$) systems, $\mu_{\text{eff-Co}}$ is directly obtained as $\mu_{\text{eff-Co}} = \mu_{\text{eff}} = \sqrt{8C}$, while in the case of the $\text{Nd}_{1-x}\text{SrxCxCoO}_3$ series the rare earth contribution to the obtained μ_{eff} has to be considered and subtracted ($\mu_{\text{eff}}(\text{Nd}^{3+}) = 3.8 \mu_{\text{B}}$).

The results obtained for the different series show that $\mu_{\text{eff-Co}}$ are in general rather similar for the $\text{La}_{1-x}\text{SrxCxCoO}_3$ and $\text{La}_{1-x}\text{CaxCxCoO}_3$ series, while they are higher in the case of the $\text{La}_{1-x}\text{BaxCxCoO}_3$ compounds and smaller in the $\text{Nd}_{1-x}\text{SrxCxCoO}_3$ system. (Fig. 2a).

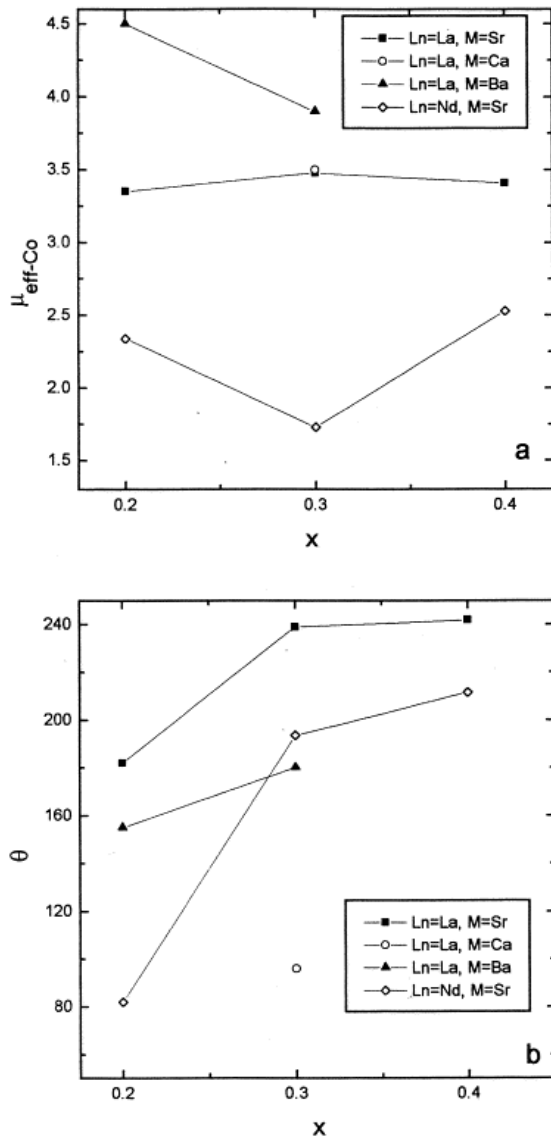


Fig. 2. (a) Effective magnetic moment per cobalt ion, and (b) Weiss constant corresponding to the $\text{La}_{1-x}\text{MxCoO}_3$ ($\text{M}=\text{Ca}, \text{Ba}$) and $\text{Nd}_{1-x}\text{SrxCxCoO}_3$ systems in the compositional interval $0.20 \leq x \leq 0.40$.

As for θ , it is seen to increase with x in all four series (Fig. 2b) so that the negative values found for lower doping degrees change to higher positive values as x gets higher, in good agreement with literature data[6] and [8].

As for the $M(H)$ curves corresponding to the ferromagnetic samples, they show that at 77 K none of them reaches saturation under a field of $H=10$ kOe (Fig. 3), even if the values of maximum magnetization increase with x in all the studied series.

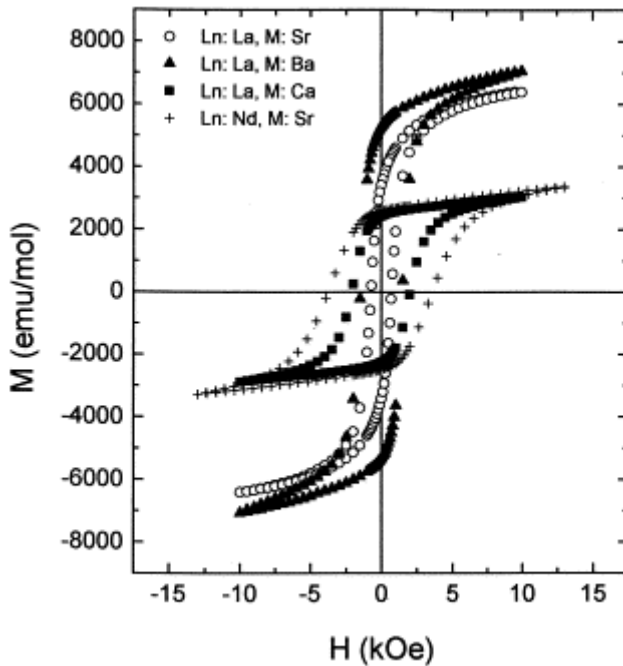


Fig. 3. ZFC magnetization M versus applied field H of $x=0.30$ $\text{La}_{0.70}\text{M}_{0.30}\text{CoO}_3$ (M: Ca, Sr, Ba) and $\text{Nd}_{0.70}\text{Sr}_{0.30}\text{CoO}_3$ samples, measured at 77 K.

If we compare $M(H)$ loops corresponding to the different $\text{Ln}_{1-x}\text{M}_x\text{CoO}_3$ systems (Fig. 3), we find that the values of maximum magnetization, extrapolated magnetization (result of the linear extrapolation of $M(H)$ for higher fields back to $H=0$) and remnant magnetization follow the sequence: $\text{La}_{1-x}\text{Ba}_x\text{CoO}_3 > \text{La}_{1-x}\text{Sr}_x\text{CoO}_3 \gg \text{La}_{1-x}\text{Ca}_x\text{CoO}_3 > \text{Nd}_{1-x}\text{Sr}_x\text{CoO}_3$.

As for the coercive field, it is remarkably higher in the $\text{Nd}_{1-x}\text{Sr}_x\text{CoO}_3$ system, where it achieves a maximum value of ≈ 3800 Oe for $x=0.30$, and then decreases to 3200 and 2400 Oe for $x=0.40$ and for $x=0.20$, respectively.

It should be noted here that the magnetic properties of these samples are not seen to experience temporal evolution, at difference with what occurs with their electrical behavior (see below).

3.3. Electrical properties

When measuring the resistivity as a function of temperature $\rho(T)$, the first general observation is that the resistivity of the samples decreases as the doping degree increases, in full agreement with results reported in the literature [8] and [20] (Fig. 4), and that a smooth transition from semiconducting to metallic behavior takes place. The doping degree at which the electrical percolation is achieved depends on the system: it is, $x=0.30$ for $\text{La}_{1-x}\text{Ba}_x\text{CoO}_3$ and $\text{La}_{1-x}\text{Sr}_x\text{CoO}_3$; $x>0.30$ for $\text{La}_{1-x}\text{Ca}_x\text{CoO}_3$; and $x>0.40$ for $\text{Nd}_{1-x}\text{Sr}_x\text{CoO}_3$.

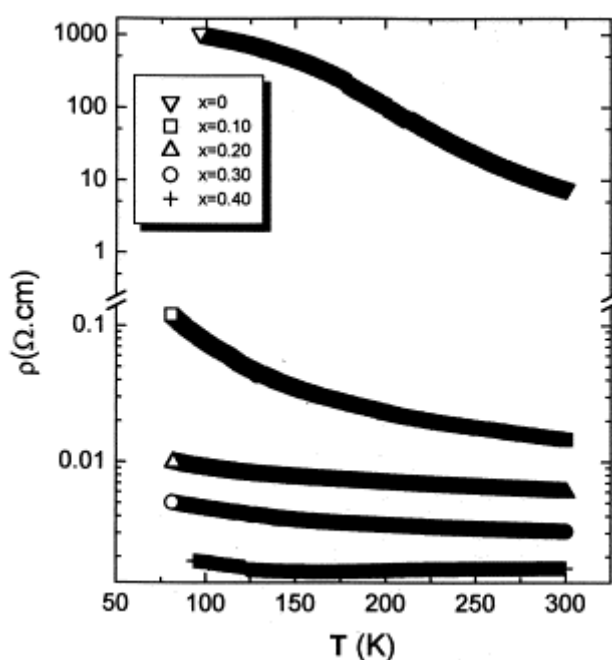


Fig. 4. Electrical resistivity versus temperature of $\text{Nd}_{1-x}\text{Sr}_x\text{CoO}_3$ samples ($0 \leq x \leq 0.40$).

Very interestingly, for compositions very close to the electrical percolation threshold, we find samples that experience M–I transitions as temperature rises. Among them, the compounds $\text{La}_{0.70}\text{Ca}_{0.30}\text{CoO}_3$, $\text{La}_{0.80}\text{Sr}_{0.20}\text{CoO}_3$, $\text{La}_{0.75}\text{Sr}_{0.25}\text{CoO}_3$ and $\text{La}_{0.80}\text{Ba}_{0.20}\text{CoO}_3$, that show I–M–I transitions, also known as a ‘reentrant semiconducting behavior’ (RSB) [7], i.e., the samples are semiconducting below a T_{MI1} and above a T_{MI2} , and metallic for $T_{\text{MI1}} < T < T_{\text{MI2}}$ (Fig. 1a–c); and the $\text{Nd}_{0.60}\text{Sr}_{0.40}\text{CoO}_3$ sample, which is semiconducting for $T < T_{\text{MI}}=160$ K and metallic above it (Fig. 1d). In this case, only a small change in the positive slope of the $\rho(T)$ curve takes place at T_c and the sample remains metallic up to room temperature.

These samples with M–I transitions are very sensitive to external influences. Although from the crystallographic and magnetic point of view the samples seem to be stable and are not seen to experience temporal evolution, their electrical resistivity does

indeed change with time. Depending on the nature and characteristics of the sample this aging takes place at a different speed, being slower for the $\text{La}_{0.80}\text{Ba}_{0.20}\text{CoO}_3$ and $\text{La}_{0.70}\text{Ca}_{0.30}\text{CoO}_3$ samples. In these cases it is possible to see the resistivity of the samples progressively increase in the interval of several weeks, until the RSB disappears giving rise to a purely semiconducting behavior in the whole temperature range [21]. $\text{La}_{1-x}\text{Sr}_x\text{CoO}_3$ ($x=0.20$ and 0.25) samples also arrive to this final situation, but much faster.

It is also interesting to note that electrical current is seen to help to that ‘aging’: after making several runs of $\rho(T)$ measurements the resistivity of the samples increases (Fig. 5), specially if the electrical current is applied only in one direction. This effect is specially important in the $\text{Nd}_{1-x}\text{Sr}_x\text{CoO}_3$ samples.

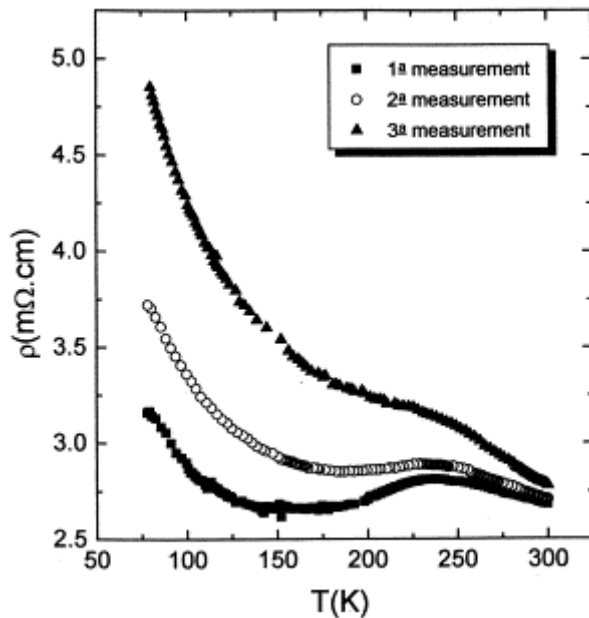


Fig. 5. Evolution of the electrical resistivity of $\text{La}_{0.80}\text{Sr}_{0.20}\text{CoO}_3$ when making several runs of $\rho(T)$ measurements.

Also, very surprisingly, the value and even temperature dependence of the resistivity are greatly affected by the polarity of the applied electrical current. For example, for $\text{La}_{0.80}\text{Ba}_{0.20}\text{CoO}_3$: $\rho^+(T)$ shows a semiconducting behavior, $\rho^-(T)$ is smaller and shows a M-I transition, ρ_{av} , measured inverting the polarity of the current, gives intermediate values and a RSB (Fig. 6).

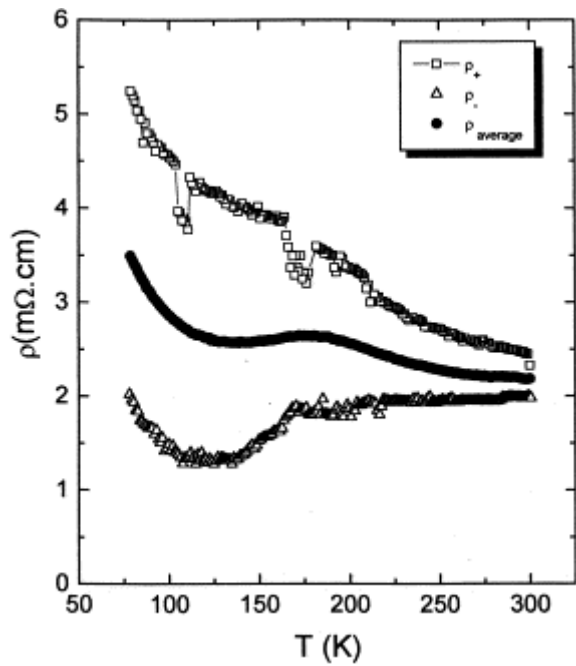


Fig. 6.

$\rho^+(T)$, $\rho^-(T)$ and $\rho(T)$ results corresponding to $\text{La}_{0.80}\text{Ba}_{0.20}\text{CoO}_3$. While the $\rho^+(T)$, $\rho^-(T)$ curves were measured using only one polarity of the current, the average $\rho(T)$ curve was obtained inverting the polarity.

We have also found that when inverting the polarity of the electrical current, the change of resistivity is not immediate but presents a highly anomalous time-dependent relaxation. For example in $\text{La}_{0.80}\text{Ba}_{0.20}\text{CoO}_3$ samples a time of about 10 min is needed in order to recover the resistivity measured before the current switch.

These samples with M-I transitions are also sensitive to the magnetic field. In this context, doped lanthanum samples with RSB show magnetoresistive effects, specially at temperatures close to T_{MI} (Fig. 7a). The typical $(\Delta R/R)$ ratio is 1–3% for the highest field used of 9 kOe (Fig. 7b), but it is worth noting that strong noise is frequently present in these measurements.

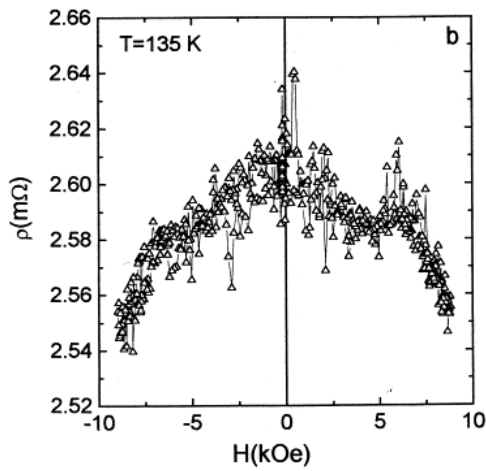
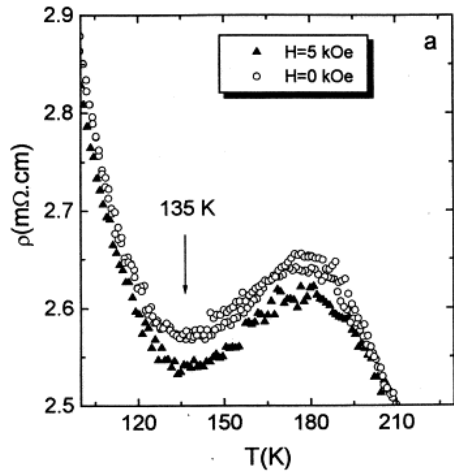


Fig. 7.

(a) Influence of a magnetic field $H=5$ kOe on the $R(T)$ curve of $\text{La}_{0.80}\text{Ba}_{0.20}\text{CoO}_3$. The arrow shows the temperature at which the magnetoresistance was measured. It is plotted in part (b) of this figure.

In the case of the $\text{Nd}_{0.60}\text{Sr}_{0.40}\text{CoO}_3$ compound, this sample shows a peculiar behavior under the application of these small magnetic fields: its resistivity keeps decreasing while sweeping the field (Fig. 8).

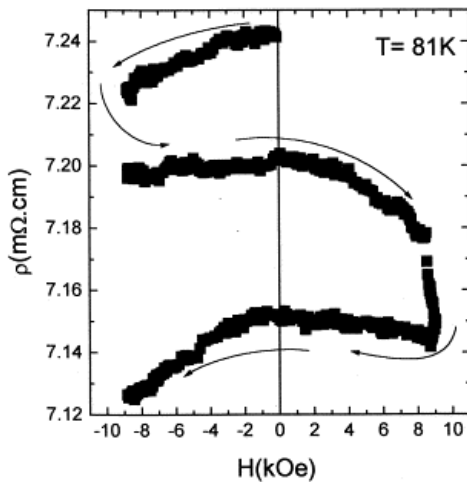


Fig. 8.

Evolution of the electrical resistivity of the $\text{Nd}_{0.60}\text{Sr}_{0.40}\text{CoO}_3$ sample under the influence of the magnetic field ($T=81$ K).

4. Discussion

The peculiar magnetic and electrical behavior displayed by these $\text{Ln}_{1-x}\text{MxCoO}_3$ series of compounds can be understood as properties of an inhomogeneous media [22] or as a result of segregation of two phases[23].

In this context, it has recently been proposed [7] that in $\text{La}_{1-x}\text{SrxCoO}_3$ there are two distinguishable electronic phases that coexist within the same crystallographic phase: one would be hole-rich, metallic and ferromagnetic, while the other would be hole-poor, semiconducting, and with AF exchange interactions, in which the Co ions are in a spin state that changes with temperature. When the ferromagnetic phase reaches the magnetic percolation threshold bulk ferromagnetism is observed below T_c . For higher x the ferromagnetic hole-rich regions also percolate from the electrical point of view, but for a compositional interval with x slightly lower than the electrical percolation threshold, the electrical conduction in the ferromagnetic regions is modulated by the mediating matrix [7].

Our electrical and magnetic results for $\text{La}_{1-x}\text{MxCoO}_3$ ($\text{M}=\text{Ca}, \text{Sr}, \text{Ba}$) and $\text{Nd}_{1-x}\text{SrxCoO}_3$ series support the idea that in the four systems two electronically different phases coexist within the same crystallographic phase, and that the model for $\text{La}_{1-x}\text{SrxCoO}_3$ can be extended to them. Of course, to do this one has to take into account that the nature and size of both the Ln^{3+} and M^{2+} cations will influence the spin-state of the Co ions in these systems [13] and [16], the values of x for magnetic and electrical percolation, T_c and the magnetic characteristics of the samples [8] and [18].

For example in the $\text{Nd}_{1-x}\text{SrxCoO}_3$ system, although magnetic percolation is achieved for $x=0.20$, electrical percolation is not reached until $x>0.40$. This could be due to the fact that as the electrical conduction is mediated by a matrix with Co ions in a relatively lower spin configuration — as indicated by the magnetic results — the connection between hole-rich regions would be more difficult [7], and would then take place for higher x .

Our magnetic results show that for each series the Curie temperature of the ferromagnetic samples changes but very little with x , and it is worth noting that a constant T_c would indicate a phase segregation. Also, for compositions near the percolation threshold a $\theta < T_c$ is found suggesting the presence of AF interactions within the ferromagnetic materials.

The electrical behavior displayed by these samples near the percolation threshold is specially revealing: if there were two electrical phases in the systems, the predominant phase would control the observed electrical behavior. Within this model the semiconducting behavior observed at low temperatures is due to the fact that the metallic regions are disconnected so that the semiconducting behavior of the other phase is observed. Between T_{MI1} and T_{MI2} (or above T_{MI1} , in the case of $Nd_{0.60}Sr_{0.40}CoO_3$), spin-state changes in the semiconducting phase allow the metallic regions to percolate. Above T_{MI2} (or T_c , in the case of $Nd_{0.60}Sr_{0.40}CoO_3$), the ferromagnetic phase becomes paramagnetic and spin-disorder scattering in this phase reduces its volume. In the case of $Nd_{1-x}Sr_xCoO_3$, this effect gives rise to a change in the slope of the $\rho(T)$ curve, that in any case remains positive, while in the case of the lanthanum-series the percolation pathways then break, and what dominates the electrical conduction is the movement of charge carriers through the semiconducting phase with an activated mobility.

Other support for the model of two electrical phases coexisting in the system comes from the relaxation effects observed when the current is changed and the 'dioidic' behavior observed in these samples. If the materials are thought of as an electrically inhomogeneous medium, where some metallic clusters are covered with a semiconducting and dielectric material, the changes in the polarity of the electrodes will affect the charge distribution in the dielectric medium. This, in turn, will change the density of charge carriers and, therefore, the resistivity of these materials, as found in other perovskite compounds [24].

As for magnetoresistance in these systems it has been reported that in the $La_{1-x}Sr_xCoO_3$ system samples with doping $0.2 < x < 0.4$ show a small negative magnetoresistance ($(\Delta R/R) < 10\%$ in a magnetic field of 6 T), while for doping degrees closer to $x=0.2$ larger values of magnetoresistance are found (up to $(\Delta R/R) \approx 40\%$ for $H=6$ T) [9] and [10]. Very recently, magnetoresistive effects have also been reported in $La_{1-x}Ba_xCoO_3$ [11] and [25].

In our case, for the doped lanthanum samples with RSB we observe a magnetoresistive response of 1–3% in a magnetic field as low as 9 kOe for temperatures near T_{MI1} and T_{MI2} . This result, that could be interpreted as the result of growth of the hole-rich ferromagnetic regions under application of the field at the expense of the poor-conducting matrix through changes in its Co-spin state, would be rather promising for the possible use of these materials as magnetic sensors if the noise did not affect the measurement so much [21].

As for the observed electrical 'aging' and evolution with time and applied electrical current of the samples with compositions near the percolation threshold, it seems to be related to small changes in their oxygen stoichiometry as revealed by preliminary oxygen content analyses (Sánchez M, Rey C, Breijo MP, Señarís-Rodríguez MA, unpublished results), by the fact that appropriate thermal treatments can restore the initial electrical behavior [25], and by results reported by authors on the evolution from metallic to semiconducting behavior of $\text{La}_{0.50}\text{Sr}_{0.50}\text{CoO}_3$ thin films [26].

Finally, it is worth outstanding note that the fact that $\text{Nd}_{1-x}\text{Sr}_x\text{CoO}_3$ samples with compositions near the critical x for electrical percolation are even more sensitive to electrical current and its polarity than the $\text{La}_{1-x}\text{M}_x\text{CoO}_3$ ($\text{M}=\text{Ca}, \text{Sr}, \text{Ba}$) series. Also, highly peculiar $\rho_T(H)$ curves suggest the existence of important relaxation effects in these samples, that seem to be related to the presence of Nd^{3+} ions. These ions, at difference with La^{3+} ions have a big orbital angular momentum ($L=6$) [27], and give rise to high magnetocrystalline anisotropy, and the observed high coercive fields, and could be involved in a richer dynamic phenomenology under the application of electrical current and magnetic fields.

More work is in progress to completely clarify these surprising and interesting effects.

Acknowledgements

We thank the Spanish DGICYT for financial support under project MAT98-0416-C03-02.

References

1. J.B. Goodenough, J.M. Longo
Landolt-Börnstein Tables, group III, 4aSpringer-Verlag, Berlin (1970)
2. R. Von Helmot, et al.
Phys Rev Lett, 71 (1993), p. 2332
3. S. Jin, et al.
Science, 264 (1994), p. 413
4. J.B. Goodenough
J Phys Chem Solids, 6 (1958), p. 287

5. P.M. Raccach, J.B. Goodenough
Phys Rev, 155 (1967), p. 932
6. P.M. Raccach, J.B. Goodenough
J Appl Phys, 39 (1968), p. 1209
7. M.A. Señarís-Rodríguez, J.B. Goodenough
J Solid State Chem, 118 (1995), p. 323
8. C.N.R. Rao, O.M. Parkash, D. Bahadur, P. Ganguly, A. Nagabhu Share
J Solid State Chem, 22 (1977), p. 353
9. V. Golovanov, L. Mihaly, A.R. Moodenbaugh
Phys Rev B, 53 (1996), p. 8207
10. R. Mahendiram, K. Raychaudhuri
Phys Rev B, 54 (1996), p. 16044
11. A. Barman, M. Ghosh, S.K. De, S. Chatterjee
Phys Lett A, 234 (1997), p. 384
12. V.G. Bhide, D.S. Rajoria, G.R. Rao, C.N.R. Rao
Phys Rev B, 6 (1972), p. 1021
13. G. Thornton, F.C. Morrison, S. Portington, B.C. Tofield, D.E. Willian
J Phys C: Solid State Phys, 21 (1988), p. 2871
14. M.A. Señarís-Rodríguez, J.B. Goodenough
J Solid State Chem, 116 (1995), p. 224
15. S. Yamaguchi, Y. Okimoto, Y. Tokura
Phys Rev B, 55 (1997), p. R8666
16. D.S. Rajoria, V.G. Bhide, G. Rama Rao, C.N.R. Rao
J Chem Soc Faraday Trans II, 70 (1974), p. 512
17. A. Cassalot, P. Dougier, P. Hagenmuller
J Phys Chem Solids, 32 (1971), p. 407
18. G. Demazeau, M. Pouchard, P. Hagenmuller
J Solid State Chem, 9 (1974), p. 202
19. M. Itoh, I. Natori, S. Kubota, K. Matoya
J Phys Soc Jpn, 63 (1994), p. 1486
20. C.N.R. Rao, O.M. Parkash
Phil Mag, 35 (1977), p. 1111
21. Mira J, Rivas J, Breijo M.P, Señarís-Rodríguez MA, Sánchez RD. Sensors Actuators A:
Physics (1998) (to be published).
22. D. Bergman, D. Stroud

Solid State Phys, 46 (1992), p. 147

23. E.L. Nagaev
Phys Stat Sol (B), 186 (1994), p. 9
24. C.H. Ahn, R.H. Hammond, T.H. Geballe, M.R. Beasley, J.M. Triscone, M. Decroux, Fisher, L. Antognazza, K. Char
Appl Phys Lett, 70 (1997), p. 206
25. R.D. Sánchez, J. Mira, J. Rivas, M.P. Breijo, M.A. Señarís-Rodríguez
J Mater Res., 14 (1999), p. 2533
26. R. Ramesh, A. Krishnan, D. Keeble, E. Poindexter
J Appl Phys, 81 (1997), p. 3543
27. S. Chikazumi
Physics of magnetism, Krieger, Malabar, FL (1986) chs. 7 and 10

Paper presented at the First International Conference on Inorganic Materials, Versailles, France, 16–19 September, 1998.